SECTION 5
CHARACTERIZING BPL EMISSIONS THROUGH COMPUTER MODELING AND MEASUREMENTS

5.1 INTRODUCTION

This section explains theoretical factors in BPL signal radiation and propagation and summarizes key findings from NTIA's measurement and modeling efforts to date (Appendix D and E). Environmental RF noise levels are discussed insofar as ambient noise is an important factor in the evaluation of interference. These considerations are applied in Section 6 in evaluations of risks of interference to representative Federal Government systems.

5.2 THEORY

5.2.1 Relevant Radiation Theory

In the subject range of frequencies, 1.7 – 80 MHz, BPL devices and the power lines that carry BPL signals have the potential to act as unintentional radiators. The amount of radiation depends on the symmetry of the network at radio frequencies. Symmetry is defined in terms of impedance between conductors and ground. If for a two wire line, the impedance between each conductor and ground is equal, the line is symmetrical or balanced. A lack of symmetry leads to an unwanted, common mode signal. Common mode currents flow in parallel in both conductors, while return portions flow through ground. Balanced lines are necessary for differential mode transmission in which currents are equal in magnitude and flow in opposite directions on the signal conductors. The fields radiating from these conductors tend to cancel each other in the far field area. On parallel or nearly parallel, non-concentric conductors, common mode currents at radio frequencies produce more radiation than differential mode currents.[37]

Any impedance discontinuity in a transmission line, which may arise from a BPL coupling device, a transformer, branch or a change in the direction of the line, may produce radiation directly or by reflections of signals forming standing waves that are radiated from the conductors. Even if the RF energy is injected into one of two or more conductors, the remaining wires generally act as parasitic radiators and, therefore, the lines can act as an array of antenna elements at certain frequencies. Radiation may come from one or more point radiators corresponding to the coupling devices as well as one or more power lines. Numerical Electromagnetics Code (NEC), as discussed later in this section, and similar method of moments models, as used with realistic physical arrangements and impedances of the power lines, have been applied to simulate the

[37] *See e.g.*, *Physical and Regulatory Constraints for Communication over the Power Supply Grid*, M. Gebhardt, F. Weinman and K. Dostert, IEEE Communications Magazine, May 2003, pp. 84-90.

current distribution on the power lines and the radiated fields. Modeling results shown in Appendix E and discussed in this section indicate that, depending on radio antenna polarization, standing waves generated by an impedance discontinuity will produce radiation at numerous points along the power lines.

The space surrounding a radiator can be divided into three regions: the reactive near-field, the radiating near field and the far field. The boundaries of the radiating near field are often given as $0.62 \cdot \sqrt{\left(D^3/\lambda\right)} < r < 2 \cdot D^2/\lambda$, where "D" is the largest linear dimension of the radiator, "r" is the distance from the radiator, λ is the wavelength, and these dimensions and wavelength are expressed in common units (typically meters). In the near-field region, also called Fresnel region, the field pattern is a function of the radial distance. Also, it should be remembered that the criteria for defining these field boundaries are not rigid and the field spatial distributions change very gradually as the boundaries are crossed.[38] Of course, "D" depends on the extent of the line responsible for most of the radiation. For most BPL applications, the victim receivers will be in the radiating near field. However, for interference through sky waves, and at distances seen by aircraft receivers, far fields are important.

5.2.2 Propagation Modes

The dominant, relevant propagation modes in the 1.7 – 80 MHz frequency range are ground wave, space wave and sky wave. The ground wave signal can be a composite of a direct wave, a ground reflected wave and/or a surface wave. For a direct wave from a point source (*i.e.*, infinitesimal D, yield essentially no near field), the received power is inversely proportional to the square of distance (r^2). If the radiator is located several wavelengths above ground, the direct wave and the ground reflected waves are considered as separate rays and the peak combined received power is inversely proportional to r^4. If the radiator is close to ground in terms of wavelength (*e.g.*, BPL below 40 MHz), it is no longer appropriate to consider separate rays. A surface wave propagates close to ground by inducing currents which flow in the ground and support (or potentially interfere with) short range communications. However, horizontally polarized surface waves are heavily attenuated, and, for any polarization, surface wave propagation exhibits substantially higher rates of attenuation with distance than the direct wave, especially at VHF frequencies (*i.e.*, above 30 MHz). In general, sky or ionospheric waves are important up to about 30 MHz, above which propagation is sporadic. Sky wave propagation may be represented by rays which are refracted and reflected from the ionosphere and is responsible for signal transmission to distances ranging from hundreds to thousands of kilometers, depending on elevation angle of the radiated field, frequency and variability of the ionosphere. The ionosphere, which ranges from about 60 to 600 km in height, acts as a low-conductivity dielectric.[39]

---

[38] *See e.g.*, Antenna Theory, Analysis and Design, C. A. Balanis, John Wiley, 1982.

[39] *See e.g.*, Propagation of Radiowaves, Edited by M. P.M Hall, L. W. Barclay and M. T. Hewitt , IEE, London, 1996.

Space wave propagation occurs on line-of-sight signal paths above the height of the power lines where surface and reflected waves are received at magnitudes much less than the direct wave magnitude. Friis, or free-space loss typically is assumed for these paths although in most cases, reflected waves (multipath effects) can yield a degree of location variability of the received signal magnitude.

To summarize, propagation mechanisms of concern for BPL emissions toward or below the power line horizon will be by ground waves. For emissions in directions above the power line horizon, the propagation may be either by space and ground waves for shorter distances or by sky waves for larger distances.

Sky waves suffer large losses mainly due to ionospheric absorption and polarization coupling losses. In a dense deployment of BPL systems, there may be aggregation of co-frequency BPL emissions toward the ionosphere. Emissions in directions above the power lines may aggregate via sky wave or via ground wave and space wave, and emissions toward or below the power lines generally may aggregate via ground wave. Preliminary modeling of power lines (Appendix E) suggests that there is relatively strong radiation in directions above the power line horizon (*i.e.*, higher than radiation toward directions below the power lines), and so, aggregation of BPL signals at locations above power lines may be more significant than at lower heights where BPL signal propagation is less efficient.

5.3 BPL MEASUREMENTS

5.3.1 Approach

During the period August to November 2003, NTIA performed measurements with a goal of quantifying key aspects of BPL signals. The measurements were conducted at three sites where BPL systems are currently deployed for testing and are serving customers. All three of the sites had BPL signals on the MV wires and two of the sites also used BPL on the LV wires. The types of measurements of fundamental emission, as detailed in Appendix D, consisted of the following:

1. Identification and characterization of BPL signals.
2. BPL signal power at locations along and near an energized line.
3. BPL signal power at various distances away from an energized line.
4. BPL signal power comparisons using peak, average and quasi-peak detectors.
5. BPL signal power at different receiving antenna heights and polarization orientations.
6. Amplitude probability distributions (APDs) of the BPL signal.

These measurements were made using NTIA's instrumented measurement vehicle and either an antenna positioned 10 meters above the ground on a telescopic mast, or 2 meters above the ground on a wooden tripod. Four types of antennas were used. A small discone antenna over a small ground plane was used to measure the electric fields above 30 MHz. Below 30 MHz, small shielded loops were used to measure the magnetic fields,

and a rod antenna over a small ground plane was used for measuring the electric fields. To measure the received power that would be seen by a mobile unit, an off-the-shelf 2.1 meter base-loaded whip antenna was mounted on the roof of a vehicle at an approximate height of 1.5 meters. The whip antennas were narrow-banded so several of them were used to cover the measurement frequencies.

5.3.2 Identification and Characterization of BPL Signals

All measurements were preceded by system calibration as described in Appendix D. At the three BPL deployments, the BPL signals were identified and analyzed by looking at the spectrum and temporal characteristics of the BPL transmission as described in the Section D.3.1.

5.3.3 BPL Signal Power Along an Energized Power Line

The measurement results for BPL signal power along an energized power line are given in Section D.3.2. The peak received power due to the electric field generated by BPL signals was measured with a rod antenna at a height of 2 meters at various points along a power line. Three mutually orthogonal components of the electric field were measured. These measurements indicate that there is a strong BPL electric field (relative to noise) along and near the BPL power line and in general, the field does not measurably decay with distance from the device (along the power lines). In at least one case, the electric field actually increased with increasing distance from the BPL device. This is thought to be due to BPL signal reflection by one or more impedance discontinuities and the generation of standing waves. In general, the location variability in the field is thought to be due to the presence of standing waves in the current distribution along the power line.

The magnetic field using a loop antenna at 2 meters height was not measurable along the power line at most locations as indicated in Section D.3.2.

The peak received power due to the electric field was measured with the whip antenna mounted on the top of a vehicle at various distances along the power lines. The results are similar to those obtained from the electric field measurements using the rod antenna.

The measurements at one site at a frequency of 32.70 MHz and at a height of 10 meters indicate that after an initial decrease of received power with increasing distance from the BPL device along the power line, the power remains at about the same level with increasing distance along the power line.

5.3.4 BPL Signal Power Away from the Energized Power Line

The measurement results for BPL signal power away from an energized power line are given in Section D.3.3. The peak received power due to the magnetic field was measured at one site with a loop antenna directly under the power line at a height of 2 meters and a weak BPL magnetic field was detected on four frequencies (4.4 MHz, 8.8 MHz, 23.8 MHz, and 28.8 MHz). At a distance of approximately 50 meters perpendicular to the power line, BPL signals were received at only 28.8 MHz. The peak received power due to the electric field away from the power line was also measured with the vertically polarized whip antenna at 4.26 MHz, 7.30 MHz and 28.78 MHz. The results indicate that there is a decrease in received power with an increase in distance from the BPL device and power line, but the decrease was not monotonic at 28.78 MHz. The received power and the manner in which it decreased with increasing distance varied substantially at different frequencies.

At the same site, the peak received power due to the vertical electric field was measured with the whip antenna on a different path at various distances from the power line. Even though the received power generally decreases with increasing distance, there are some amplitude oscillations. This non-monotonic behavior is thought to be mainly due to near-field effects and not ground reflections; however, underground power lines that branched from the BPL transmission line were noted to run across the measurement path in the vicinity of a local peak measured signal power level.

The whip antenna was used to measure peak received power due to the vertical electric field at two other sites. At one site, the signal decreased to an immeasurable level within 600 feet. At the second site, comprising a complex arrangement of power lines with many turns and BPL devices, the signal power significantly exceeded the noise power beyond 1,500 feet (approx. 500 m).

Measurements were also conducted using a discone antenna with vertical polarization at a height of 3.4 meters above ground in another power line configuration. Pulse power measurements were made at three different frequencies (35.05 MHz, 39.93 MHz and 45.40 MHz) at various distances from the power line. In this case, the results indicate that the received power decreases as distance from the power line (r) increases at a rate lower than would be predicted by $1/r^2$ (space wave loss).

5.3.5 Measurement of BPL Using Various Detectors

Two sets of measurements were made to compare effects of using three different detectors: peak, average and quasi-peak. The results are provided in Table 5-1.

Table 5-1: Measured peak, average and quasi-peak levels

Frequency	Peak	Average	Quasi-Peak
22.96 MHz	-74 dBm	-81 dBm	-76 dBm
28.30 MHz	-60 dBm	-65 dBm	-65 dBm

5.3.6 Measurement of BPL Using Different Antenna Heights

Measurements of BPL emissions from MV lines were performed using two different antenna heights. The results show that in general, the measured power levels were substantially higher at the greater antenna height. For example, the 100% duty cycle power measured at a frequency of 32.70 MHz and at a 10 meter antenna height was 4.8 to 10.7 dB greater than at 2 meters. The pulse power at a 10 meter antenna height for this same frequency was 8.2 to 15.1 dB higher than at 2 meters.

Measurements were also made of emissions from a LV power line carrying BPL signals from a LV coupler near a pole-mounted transformer to a house (Section D.3.5). The phase lines were twisted about the neutral line. A loop antenna was oriented to maximize the reception of the horizontal magnetic field. The antenna was located at 8.7 meters from the utility pole near the midpoint of the LV line and measurements were made at antenna heights of 2 meters and 10 meters at frequencies of 5 MHz, 6.43 MHz, 10.74 MHz and 18.38 MHz, each with resolution bandwidths of 3 kHz, 10 kHz and 30 kHz. The results indicate that measured power at a 10 meter height is always larger than the power measured at 2 meter height (by 3-9 dBm). Table 5-2 summarizes results from both these measurements for 100% duty cycle power where meaningful comparisons could be made.

Table 5-2: Measured 100% Duty Cycle Power at Two Different Antenna Heights

Frequency	Bandwidth	2 meter height	10 meter height	Difference
6.43 MHz	3 kHz	-113.3 dBm	-108.7 dBm	4.6 dB
6.43 MHz	10 kHz	-109.1 dBm	-106.4 dBm	2.7 dB
18.38 MHz	3 kHz	-115.3 dBm	-106.6 dBm	8.7 dB
32.70 MHz	30 kHz	-101.1 dBm	-96.3 dBm	4.8 dB
32.70 MHz	10 kHz	-111.4 dBm	-100.7 dBm	10.7 dB

5.3.7 Measurements of BPL Amplitude Probability Distributions (APDs)

Several APDs were measured at two of the three BPL deployment sites and the results are given in Section D.3.6. At one site, APD measurements were conducted at two frequencies, 32.70 MHz and 42.47 MHz, at three different resolution bandwidths: 200 kHz, 30 kHz and 10 kHz. A discone antenna with vertical polarization located at 10 meters above the ground and 11.6 meters from the power line was used to measure the APDs and the 100% duty cycle power levels were derived from the APDs. The results

show that the 100% duty cycle power is higher for higher resolution bandwidth for the same frequency, and that the power levels are proportional to bandwidth (confirming that 100% equivalent power was accurately estimated from APDs).

With BPL loaded on the power lines, pulse-power measurements and APDs were conducted at 32.70 MHz with two different resolution bandwidths (30 kHz, and 10 kHz) and four different antenna orientations. A discone antenna was located at various direct distances from the power lines and backhaul point (*x* and *y* respectively) and set at a vertical height from the ground of 2 meters. The results indicate that the measured power for all four antenna orientations was at similar levels for the same location. A long wire antenna is linearly polarized, but the direction of the linear polarization is not the same in all parts of the pattern.[40] Therefore, in this case, similar power was measured for one set of coordinates, whereas, for another set of coordinates, the measured power for vertical polarization was larger than that for horizontal polarization.

The occasional sampling of environmental noise power levels shown in APDs with the BPL system turned off were lower than the levels predicted by ITU-R Recommendation P.372-8. Thus, the sites for these measurements have relatively low noise power levels and use of the higher noise power levels predicted by ITU-R Recommendation P.372-8 in our analyses may bias results toward underestimation of interference levels.

5.4 ANALYTICAL MODELS OF POWER LINE RADIATION

5.4.1 Numerical Electromagnetics Code (NEC)

NEC is a computer program for analyzing the electromagnetic response of antennas and scatterers.[41] The code is based on the numerical solution of integral equations by the method of moments. An electric field integral equation (EFIE) is used for modeling thin wires and a magnetic field integral equation (MFIE) is used for closed conducting surfaces. This form of simulation breaks the structure of interest down into *moments* or line segments (for solid structures, a wire mesh is used). The current in each segment is calculated and the resulting electromagnetic fields are derived.

NEC 4.1 is the latest version of the NEC, which has been developed and improved over the years at Lawrence Livermore National Laboratory. NEC codes offer features, which include excitation by voltage sources or plane waves, lumped or distributed loading, and networks or transmission lines. The code output includes current distributions, impedances, power input, dissipation, efficiency, radiation patterns, gains and scattering cross section. Among other output, it can be used to produce far-field

[40] *See e.g.*, Antenna Theory, Analysis and Design, C. A. Balanis, John Wiley, 1982, Chapter 9.

[41] Numerical Electromagnetics Code – NEC-4 Method of Moments, Part I: User's Manual, Part II: NEC Program Description - Theory, Part III: NEC Program description – Code, Gerald J. Burke, January 1992.

(power gain) antenna patterns, near-field electric and magnetic field strength, ground-wave field strengths at different distances from an antenna, antenna input impedance and total radiated power. NEC-4.1 can be used to model structures over a ground surface with a wide range of characteristics, insulated wires, impedance and conductivity in loads and wires, and various forms of electromagnetic excitation in a structure, and structures in dielectric media other than air. However, it is important to design and input the physical model correctly, precisely portraying parameters such as segment length, diameter, and wire spacing, insofar as these parameters greatly influence results in many cases. It is important that segment length be small enough that the model is well-behaved (converges) and results change little despite further shortening of the segments.

The most relevant limitation of NEC simulation for the purposes of studying BPL is the computer Random Access Memory (RAM) and computational time necessary to simulate very large structures. Computer memory needed to simulate a structure is directly proportional to the square of the number of line segments used in the structure model, as the calculations are run in a matrix. Because segment length is dictated in part by the frequency of interest, the number of line segments needed to simulate a part of a power grid can be very large. The time required to fill and factor the matrix can also become very large, depending upon the number of segments. Additionally, running a NEC simulation can become prohibitively time-consuming if the size of the matrix becomes so large that the computer's core memory is insufficient, and disk swapping occurs.

5.4.2 Modeling of Power Lines by NEC

Extensive work was done at NTIA's Institute for Telecommunication Sciences (ITS) on a typical arrangement of three phase MV power lines.[42] The modeled power lines consisted of three horizontal parallel copper wires 8.5 meters (27.9 feet) above a ground with average characteristics (conductivity σ = .005 mS, relative permittivity ε_r = 15). Each wire had a diameter of 0.01 meter (approximating AWG gauge 4/0) and the wires were separated in the horizontal plane by 0.60 meter. The feed point was at the center of one of the wires, which ran parallel to the x axis (y = 0). The equivalent of a BPL coupler was placed on the center segment of the wire and was modeled as a voltage source of 1 volt in series with a resistor that represented the source impedance. The other two phase wires ran parallel to the x axis at y = 0.6 and y = 1.2 meters.

All three orthonormal components of electric and magnetic field intensities (E_x, E_y, E_z in dBμV/m, H_x, H_y and H_z in dBμA/m) in the near field were plotted in a plane two meters above the ground at frequencies of 2 MHz, 10 MHz, and 40 MHz. Three different line lengths of 100 m, 200 m and 340 m were used with four different impedance conditions for the source and loads. The impedance conditions were as follows: source impedance of 150 Ω with load impedance of 50 Ω and 575 Ω, and

[42] *See* The Lineman's and Cableman's Handbook, E. B. Kurtz and T. M. Shoemaker, Fifth Edition, McGraw Hill, 1976.

source impedance of 575 Ω with 50 Ω and 575 Ω load impedances. The field strengths were plotted as contours in 5 dB increments for four different ranges of x and y coordinates, *i.e.*, 0 to 20 m, 0 to 200 m, 0 to 1000 m and 0 to 18000 m. The far field radiation patterns were also plotted at several azimuth angles.

Several representative far field radiation patterns and near field plots for three components of the electric field E_x, E_y and E_z are presented in Appendix E for various combinations of line length, frequency, source impedance and load impedance. The complete results of the above simulation work are available at NTIA.

The far field patterns indicate that there are more lobes in the radiation pattern as the ratio of line length to wavelength (L/λ) increases. Varying source and load impedances have minor effects. The transmission line analyzed here has a characteristic impedance of approximately 575 Ω, therefore, when the load and source impedance are both 575 Ω, the line acts as a traveling wave antenna. The highest radiation was generally associated with the combination of source impedance of 150 Ω and load impedance of 50 Ω which corresponds to the largest mismatch among the cases considered here. In the azimuth angle of 0º, *i.e.*, along the direction of the power lines, the elevation pattern has several lobes and the largest lobe is generally around 30º or lower elevation above the horizontal plane containing the power lines. The larger the L/λ ratio, the lower is this main elevation angle. However, as the azimuth angle increases to 90º, there are fewer lobes and the maximum gain is in or near the vertical direction.

Tables E-1, E-2 and E-3 summarize the results of the near field plots at 2 meters above the ground for three components of the electric field for various combinations of input parameters. Several general trends can be seen from the near field plots at 2 meters from ground near a typical power line configuration. Table E-1 summarizes the characteristics of the vertically polarized electric field, E_z. For the vertical electric field E_z, the peak field is never at the BPL source; instead, 2 to 20 local peaks occur near and under the power lines. The first peak occurs at approximately λ/4 down the wire from the device. Several peaks of slightly higher strength occur down the wire at λ/2 intervals. The number of peaks depends on the L/λ ratio. As frequency increases, the peak decreases, but the number of local peaks along the line increases. The peaks gradually diminish down the line because of RF attenuation and radiative losses. As mentioned earlier, varying source and load impedances has only a minor effect on peak field strength (less than 5 dB min-max variation), and peaks generally decrease as the source & load impedances are changed as follows (in decreasing order of peak vertical electric field strength): 150 & 50 Ω, 150 & 575 Ω, 575 & 50 Ω, 575 & 575 Ω.

Tables E-2 and E-3 summarize characteristics of horizontally polarized electric fields E_x and E_y. The peak horizontally polarized field is never at the BPL source for the perpendicular case (as was the case for vertical polarization); instead, 2 to 24 local peaks occur at various distances from the BPL source with the first peak occurring at approximately 0.75λ and subsequent peaks occurring at approximately λ/2 intervals occurring at about λ/4 on either side of the wire. In contrast, the peak field is always at

the BPL source for the parallel case with additional peaks down the line of equal or lower field strengths.

The far field patterns, the near field surface plots and measurements along power lines indicate that there are standing waves along the power line. Various other representative power line configurations need to be studied with sensitivity analysis with respect to line length, position of the source, position of other conductors in the vicinity, source and load impedances and frequency need to be done. Electric fields at other heights have to be calculated. Limited measurements have indicated that the electric fields at 10 meter high antenna are much higher than that at 2 meter high antenna. To facilitate further investigations, NTIA is developing software for statistical analysis of the spatial distribution of electric field strength.

5.4.3 Effects of a Neutral Line

In the case of power line simulation for a BPL system, the most obvious consideration is the addition of parallel wires, such as a neutral (assuming the three-phase lines are arranged in a "wye" configuration) and telephone and cable wires, which are typically found under the neutral. To determine the effects of a neutral line on the model considered above, sample simulations with and without a neutral wire were run and the resulting outputs compared to one another.

As can be seen in Figure 5-1 for a frequency of 4 MHz, the addition of a grounded neutral line does have an impact on the model output. This impact is dependent upon frequency, and primarily manifests itself in amount of gain found in the main lobes of the far-field radiation pattern. The change in gain is less than 2 dB, and the overall shape of the radiation pattern remains the about the same. The comparisons for frequencies 15 MHz, 25 MHz and 40 MHz are given in Appendix E, showing that the change in gain becomes less at higher frequencies. Equally importantly, at all of the frequencies examined, the addition of a neutral tended to *increase*, not *decrease*, the overall gain of the power line radiation. Additional computations of electric field magnitude also demonstrated an increased electric field around the modeled power line in the presence of a multi-grounded neutral. This would seem to indicate that the omission of a grounded neutral from the NEC power line model would tend to produce a more conservative result, *i.e.*, produce less radiation.

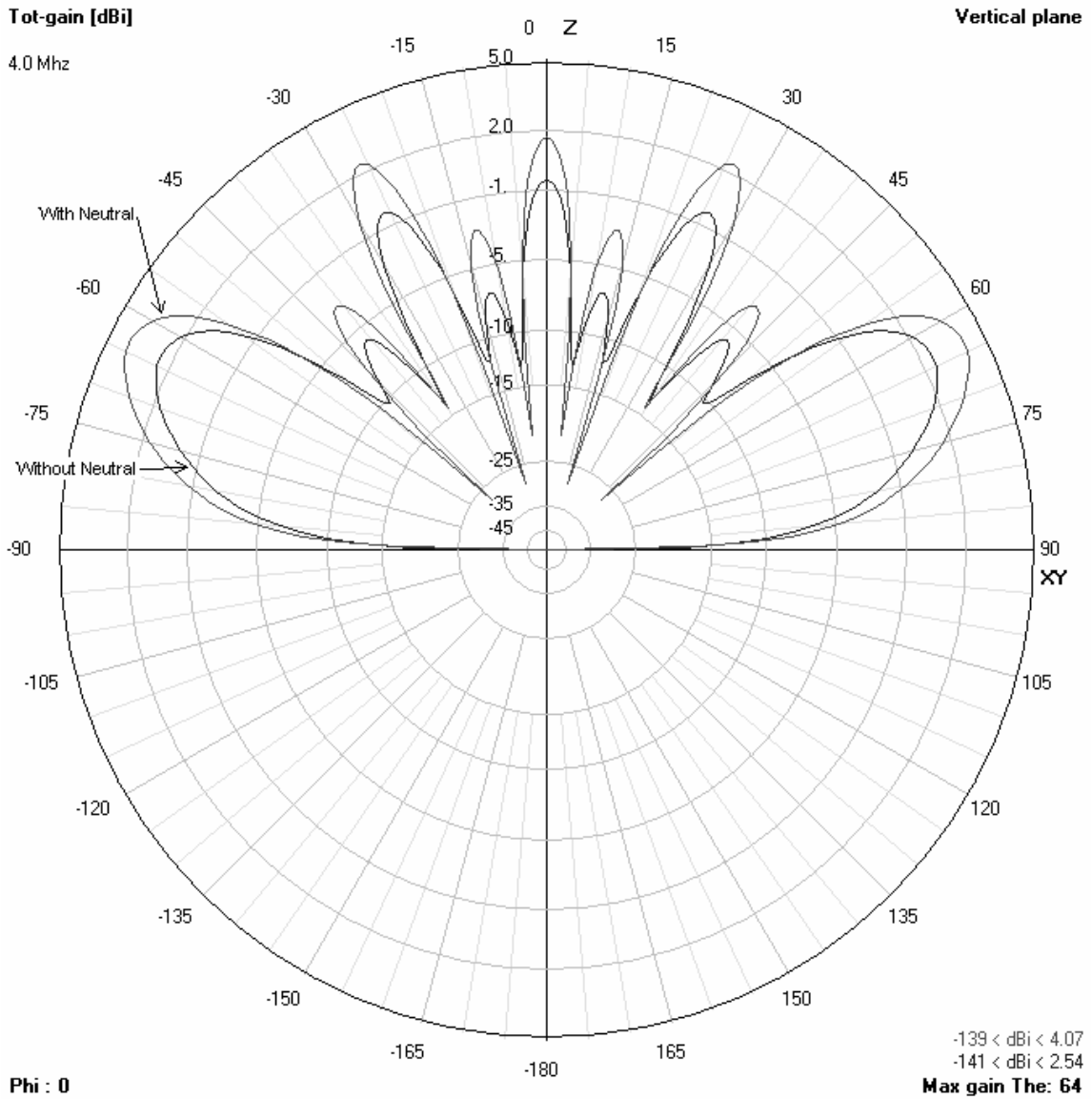

Figure 5-1: Comparison of NEC model with and without a parasitic multi-grounded neutral at 4 MHz.

5.4.4 Environmental Noise

The standard reference for radio-frequency noise is the ITU-R Rec. P.372-8. It includes detailed formulas and charts for predicting median ambient noise at any geographic point due to atmospheric, man-made and galactic noise sources as well as temporal variability. The noise at any given location varies hourly, daily, and seasonally, and predicted levels depend upon frequency, time of day, time of year and the local environment (ranging from industrial to quiet rural conditions).

Noise is especially at issue on lower frequencies in the 1.7 – 80 MHz range, because total ambient noise generally increases as the frequency decreases. In general, the level of ambient noise (the "noise floor") determines the strength of the received signal necessary to carry out communications in the absence of interfering signals. Substantial noise can make HF communications difficult or even impossible, depending upon the strength of the received signal.

The causes of HF radio noise are broadly categorized into man-made, atmospheric, and galactic sources. Each contributes to the overall noise level, and the relative contribution of each source of noise is dependent upon several factors.

Man-made noise is generally produced by electrical devices, ranging from overhead power lines to automobile ignition and household appliances. The level of man-made noise, as statistically characterized, is mainly a function of the area. Industrial areas, for example, tend to have much higher levels of man-made noise than remote rural areas. ITU-R Rec. P.372-8 specifically categorizes areas as business, residential, rural and quiet rural noise environments, in order of decreasing median noise levels. Man-made noise tends to have greater levels at higher frequencies in the 1.7 – 80 MHz range (*e.g.*, typically, above 20 MHz), although this is not always the case for all environments.

Atmospheric noise is primarily produced by lightning. Trends in this form of noise are heavily dependent upon geographic location, time of day and time of year. Areas in the Midwestern United States, for example, tend to see much higher atmospheric noise levels in the afternoon during spring and summer than do other parts of the country. Atmospheric noise tends to account for the bulk of noise at lower HF frequencies.

Galactic noise is radio noise produced by emission from celestial bodies (*e.g.*, stars) in our own galaxy, and tends to become a factor only at higher frequencies and low-noise locales. Galactic noise can serve as an effective "best case" noise level for low-noise conditions, as its level is fairly constant at a given frequency and substantial in relation to relatively low median levels of atmospheric and man-made noise.

The data in ITU-R Rec. P.372-8 is incorporated into software available from the ITU web site; that software was used in this report to obtain ambient background noise values for use in interference analyses.[43]

Noise levels have high location (spatial) variability in addition to temporal variability. For example, a business location in the Midwest United States during a summer afternoon can experience relatively high levels of noise, but a rural locale in Alaska on a winter morning can see low noise levels approaching that of the galactic background noise (Figure 5-2).

[43] NTIA's *NOISEDAT* program is available from the ITU web site, URL: http://www.itu.int/ITU-R/software/study-groups/rsg3/databanks/ionosph/index.html.

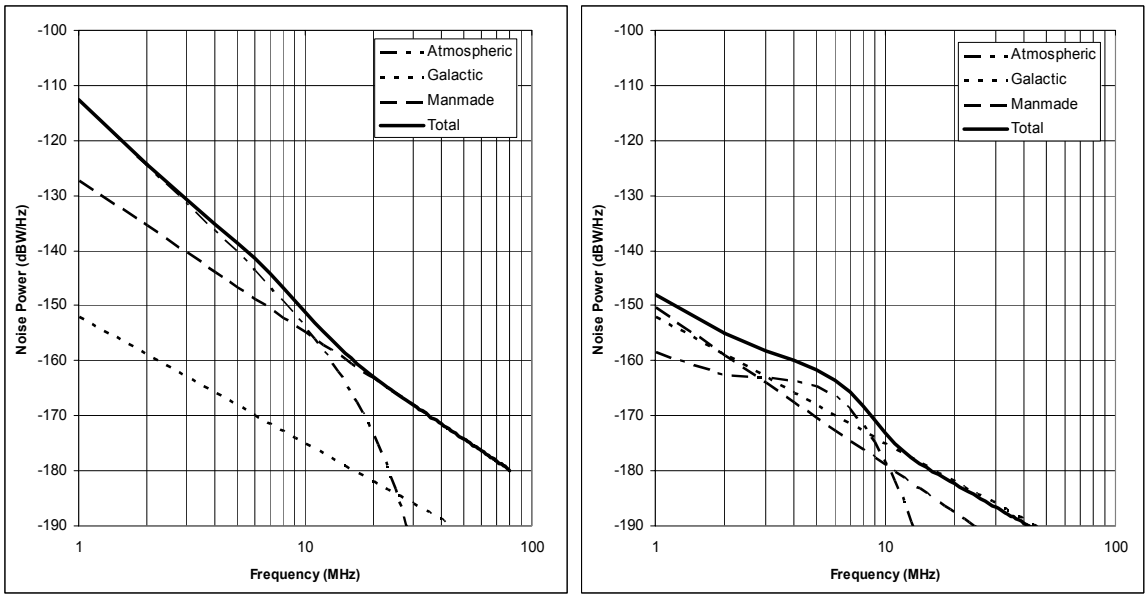

Figure 5-2: Example calculated median background noise levels. Left: industrial environment during the height of thunderstorm season in the Midwest United States. Right: rural Alaskan environment during the winter.

It is instructive to examine typical median noise values in relation to signals meeting FCC Part 15 limits. For the 1.7 - 80 MHz frequency range, Figure 5-3 and Figure 5-4 show typical median levels of receiver system noise power as well as Part 15 field strength limits at the specified measurement distance. For this figure, the noise levels were calculated for 450 locations around the United States assuming a residential environment, and the median of these values for midday in spring were selected. Several geographic points had calculated median noise values that were very close to the overall medians for each frequency; the noise levels for one such point (Kansas City, MO) were used for further calculations in Section 6.

The levels have been translated into electric field strength levels, and both the noise and the Part 15-limit electric field strength levels are presented, assuming they are received by a short vertical monopole antenna. Noise levels shown also include a 12 dB receiver noise factor, referenced to the electric field at the antenna, which (for the most part) is insignificant in relation to the ambient noise levels in question. As can be seen by the figures, signals received at Part 15 limits are 15 dB to 25 dB above the median noise levels.

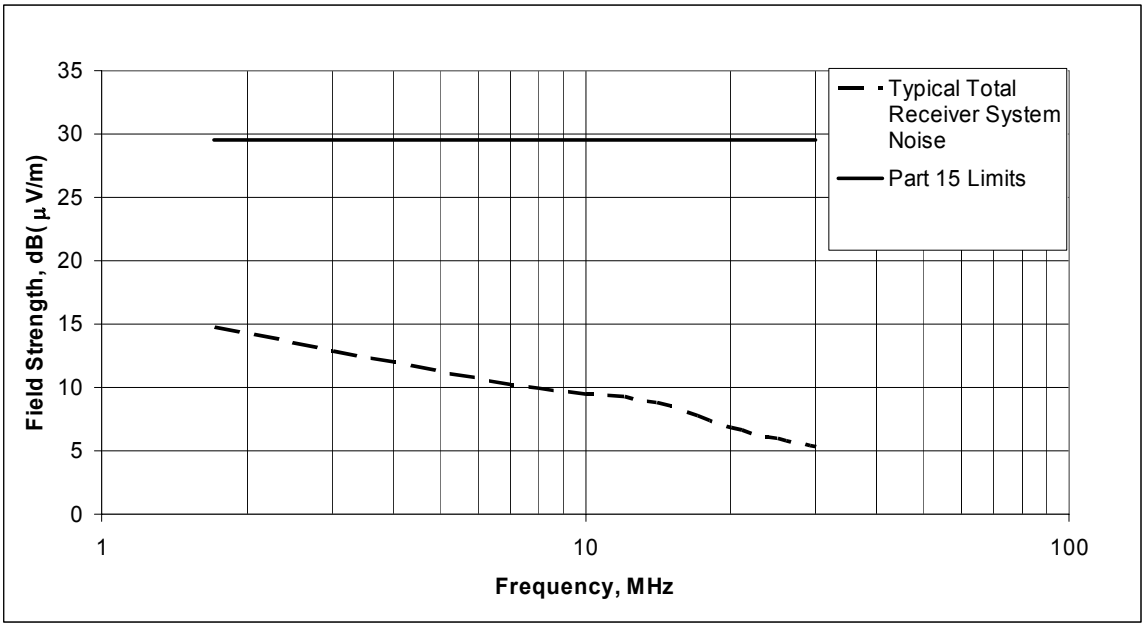

Figure 5-3: Typical median noise field strength and FCC Part 15 limits at 30 meters, 1.705 MHz to 30 MHz, 9 kHz bandwidth.

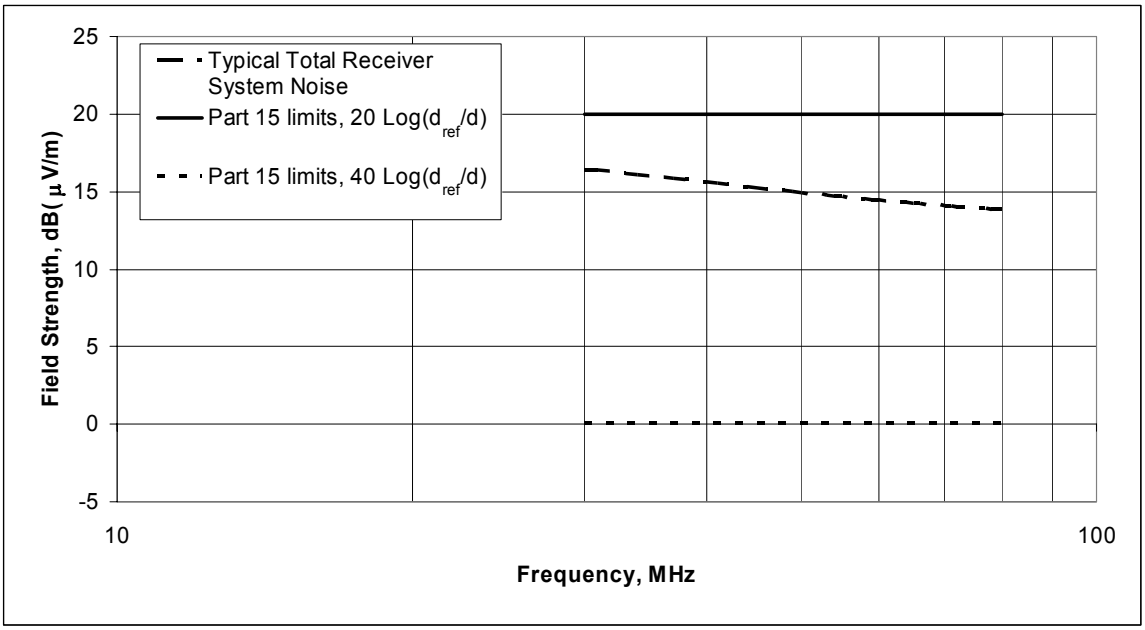

Figure 5-4: Typical median noise field strength and FCC Part 15 limits at 3 meters

5.5 CONCLUSION

Numerous textbooks explain the electromagnetic theory behind wires serving as transmission lines or antennas. For unshielded wires such as power lines, the magnitude of radiation is largely affected by the degree of balance between radio frequency currents in adjacent wires and the spacing of those wires. Common mode currents (traveling in the same direction) in parallel wires generally produce mode radiation than differential currents (traveling in opposite directions) because for differential currents, the fields generated by each wire tend to cancel if the wires are closely spaced (*e.g.*, twisted pair used for telephone lines). Impedance discontinuities can occur on power lines at transformers, branches and turns, and can produce radiation directly or cause signal reflections in the power lines that produce standing waves and associated radiation along the line. The fields generated by radio frequency currents have different types of spatial distributions in three successively more distant areas around a radiator: the reactive- and radiative-near-field and far-field regions. The distances over which reactive and radiative near-field regions extend increase with the size of the radiator and frequency. In the far field region, which could start several kilometers away from a radiating power line, the radiation patterns are independent of distance and field strength in free space generally decreases in proportion to increasing distance.

The dominant signal propagation modes in the 1.7 – 80 MHz frequency range are ground wave, space wave and sky wave. The ground wave signal can consist of a direct wave, ground reflected wave and/or a surface wave, each of which exhibit a different characteristic relationship between signal loss and distance. The direct wave signal power from a point source (*i.e.*, very small in relation to wavelength) is inversely proportional to the square of the distance and when combined with a strong ground-reflected wave from a radiator several wavelengths above the ground, the composite signal power is inversely proportional to distance to the fourth power. The latter high rate of attenuation does not occur for radiators closer to the ground. A surface wave propagates close to the ground and exhibits substantially higher rates of attenuation than the direct wave. Thus, groundwave propagation is pertinent on BPL signal paths below the power line horizon. Space wave propagation involves only a direct wave and occurs over elevated signal paths, *e.g.*, on signal paths above the power line horizon. Sky wave propagation also occurs above the power line horizon and most consistently at frequencies between 1.7 MHz and 30 MHz. Skywave signal paths are represented as rays that are refracted and reflected by the ionosphere and can extend to distances of thousands of kilometers depending on the signal elevation angle and frequency as well as parameters of the ionosphere that exhibit temporal and spatial variability.

As a part of its study, NTIA modeled an overhead, three-phase MV power line using the NEC software program. The far field patterns of the electric field indicate that there are more local peaks in the radiation pattern as the ratio of line length to BPL signal wavelength increases. Varying the source and load impedances have a minor effect, although the highest radiation was generally associated with the largest impedance mismatch between source and load. The far field radiation patterns and radiating near-

fields at a height of two meters both indicate that BPL signal reflections from impedance discontinuities can generate standing waves that cause radiation from power lines. Along the direction of the power lines, the peak field strength in the far field occurs above the horizontal plane containing the power lines. In the near field, the peak level of the vertical electric field is never at the BPL source; instead, multiple local peaks occur near and under the power lines. Similarly, the peak horizontally polarized field in the direction perpendicular to the power lines is never at the BPL source; instead, peaks occur at various distances away from the BPL source and power lines. Based on the models considered to date, only in the case of the horizontally polarized electric field in the direction parallel to the power lines does the peak field occur at the BPL device. NTIA's modeling showed that inclusion of a neutral line with three phase medium voltage wiring tended to increase the overall radiation. Thus, models omitting the neutral wire tend to predict lower field strength. The implications of these modeling results are that compliance measurements taken only around a BPL device and at heights below the power lines, may significantly underestimate the peak electric field.

NTIA performed measurements at three different BPL deployment sites in order to characterize the BPL fundamental emissions. Measurements indicate that the BPL electric field does not generally decay monotonically with distance from the BPL source as the measurement antenna was positioned near to and moving along the length of the power line. As the measurement antenna was moved away from the BPL energized power line, the radiated power decreased with increasing distance, but the decrease was not always monotonic and a number of local peaks were observed at some locations. In some cases, the BPL signal was observed to decay with distance away from the power line at a rate slower than would be predicted by space wave loss from a point source. At one measurement location where a large number of BPL devices were deployed on multiple three-phase and single-phase MV power lines, appreciable BPL signal levels (*i.e.*, at least 5 dB higher than ambient noise) were observed beyond 500 meters from the nearest BPL energized power lines. Finally, NTIA's measurements show that the radiated power from the BPL energized power lines was consistently higher when the measurement antenna was placed at a greater height (*e.g.*, 10 meter vs. 2 meter). These results indicate a need to refine the Part 15 compliance measurement guidelines to ensure that the peak field strength of any unintentional BPL emissions is measured.